APL Materials

Research Update: Van-der-Waals epitaxy of layered chalcogenide Sb_2Te_3 thin films grown by pulsed laser deposition

Cite as: APL Mater. **5**, 050701 (2017); https://doi.org/10.1063/1.4983403
Submitted: 31 January 2017 • Accepted: 01 May 2017 • Published Online: 15 May 2017

Isom Hilmi, Andriy Lotnyk, Jürgen W. Gerlach, et al.

Research Update: Van-der-Waals epitaxy of layered chalcogenide Sb_2Te_3 thin films grown by pulsed laser deposition

Isom Hilmi,[1,a] Andriy Lotnyk,[1] Jürgen W. Gerlach,[1] Philipp Schumacher,[1] and Bernd Rauschenbach[1,2]
[1]*Leibniz-Institut für Oberflächenmodifizierung (IOM), 04318 Leipzig, Germany*
[2]*Universität Leipzig, Felix-Bloch-Institut für Festkörperphysik, 04103 Leipzig, Germany*

(Received 31 January 2017; accepted 1 May 2017; published online 15 May 2017)

An attempt to deposit a high quality epitaxial thin film of a two-dimensionally bonded (layered) chalcogenide material with van-der-Waals (vdW) epitaxy is of strong interest for non-volatile memory application. In this paper, the epitaxial growth of an exemplary layered chalcogenide material, i.e., stoichiometric Sb_2Te_3 thin films, is reported. The films were produced on unreconstructed highly lattice-mismatched Si(111) substrates by pulsed laser deposition (PLD). The films were grown by vdW epitaxy in a two-dimensional mode. X-ray diffraction measurements and transmission electron microscopy revealed that the films possess a trigonal Sb_2Te_3 structure. The single atomic Sb/Te termination layer on the Si surface was formed initializing the thin film growth. This work demonstrates a straightforward method to deposit vdW-epitaxial layered chalcogenides and, at the same time, opens up the feasibility to fabricate chalcogenide vdW heterostructures by PLD.
[http://dx.doi.org/10.1063/1.4983403]

Phase change materials (PCMs) are one of the most promising materials for applications in non-volatile data memories. Amongst them, chalcogenide alloys are considered as a prospective material.[1] Recently, it was shown that it is possible to stack two different thin layers of PCMs, resulting in a specifically designed material. This artificial structure is constructed out of layers of different chalcogenides, commonly using GeTe and Sb_2Te_3 as starting materials.[2] That structure, referred to as a van-der-Waals (vdW)-chalcogenide heterostructure,[3] theoretically features crystalline layers intercalated by quasi-vdW gaps. Through the commonly believed solid-to-solid switching mechanism,[2,4] this structure of $(GeTe)_x$-$(Sb_2Te_3)_y$ has been shown possessing remarkable improvements in device performance, in terms of power efficiency and stability.[2,5] Additionally, improvement was also reported in its magnetic properties.[6] Hence, the recent research on chalcogenide PCMs is mainly focused on exploring vdW heterostructures.

With the aim to fabricate the vdW-chalcogenide heterostructure, efforts are also being put to deposit high quality epitaxial thin films of Te-based layered (2D) materials. Beside many methods,[7–10] the epitaxial deposition of layered chalcogenides is to date mainly done by molecular beam epitaxy (MBE).[11,12] However, intricate substrate's surface preparations prior to epitaxial deposition is prerequisite, i.e., surface reconstruction of Si and passivation of the Si surface by a chalcogen or pnictogen layer (such as Se, Sb, or Bi).[11–15] Moreover, a concern on stoichiometric preservation has also been reported in the grown chalcogenide films.[14,16,17] This is mainly due to a high vapor pressure and a low sticking coefficient of chalcogens (i.e., Se or Te) at elevated temperature.[14,16–18] Hence, a more straightforward method to fabricate good quality epitaxial layered materials is sought. In this case, pulsed laser deposition (PLD) offers some advantages in scientific and industrial points of view. PLD

[a]isom.hilmi@iom-leipzig.de

is capable of providing a stoichiometric transfer from the complex chemical composition of target to the substrate.[10,19,20] By PLD, epitaxial layered chalcogenide thin films with a complex chemical composition, i.e., stoichiometric Ge-Sb-Te (GST) thin films, has also been successfully deposited on Si with a high deposition rate.[19–21] Moreover, PLD has been successfully used to deposit other 2D materials.[22–25] Additionally, highly oriented poly-Sb_2Te_3 films were also deposited on various substrates by PLD.[10,26]

In this paper, van-der-Waals epitaxy of layered chalcogenide thin films grown by PLD is demonstrated. Sb_2Te_3 is chosen as a model for a layered chalcogenide material. The vdW-epitaxy is formed on Si during Sb_2Te_3 deposition, without any surface pre-treatment to deactivate Si dangling bonds. Besides its crucial role as one component in vdW-chalcogenide heterostructures,[2,5,6,27,28] as a thin film Sb_2Te_3 is also prospective for many applications, such as in the field of topological insulators (TIs)[29,30] or thermoelectric devices.[31–33] Sb_2Te_3 crystallizes in a trigonal crystal system with the space group R-3mH as many layered Ge-Sb-Te crystal structures.[34] It consists of stacked quintuple layer (QL) building blocks along the c-axis, intercalated by a quasi vdW gap. Meanwhile, Si (lattice mismatch to Sb_2Te_3 of 11%) is the common substrate in microelectronics. The growth of high quality epitaxial layered materials on standard substrates like Si is scientifically and industrially intriguing. This work also opens up the feasibility of further development in fabrication of chalcogenide superlattices by PLD.

High quality epitaxial Sb_2Te_3 thin films were deposited on a clean non-reconstructed Si(111) surface. The wet chemical cleaning process of substrates was done prior to the film deposition and is detailed in Refs. 19 and 20. The clean substrate was loaded into the chamber and heated to the desired deposition temperature T_s. Before starting the deposition, the substrate was kept at T_S for 30 min. T_s was varied for each deposition from RT to 280 °C. The temperature calibration is described in detail in Ref. 20. The thin film depositions took place in Ar ambient gas of less than 5×10^{-3} Pa (background pressure of around 2×10^{-6} Pa). The target bulk material with a chemical composition close to Sb_2Te_3 was ablated by a KrF excimer laser beam (wavelength is 248 nm) and deposited on the Si surface positioned in a distance of 6 cm from the target surface. The laser fluence, laser repetition frequency, and number of pulses used for all the depositions of the films were ~0.8 J/cm^2, 2 Hz, and 7200, respectively. The reflection high energy electron diffraction (RHEED) system was used to monitor the *in situ* film growth. The electron beam was targeted in Si$\langle 1\bar{1}0\rangle$ direction, using a small incident angle of 2° with respect to the substrate surface. The electrons were accelerated with a voltage of 30 kV. After the Sb_2Te_3 deposition was completed, the film was naturally cooled down to RT. An amorphous $LaAlO_x$ layer with a thickness of ~8 nm was then deposited on top of the film as a capping layer, in order to protect the film from oxidation during ambient storage. The crystalline quality of the thin films was assessed by x-ray diffraction (XRD) methods. All XRD based measurements were carried out using Cu-K_α radiation in a parallel beam geometry. In order to suppress Cu-K_β contributions, a graphite monochromator was attached. The film thicknesses were measured and confirmed by x-ray reflectivity (XRR) and cross section scanning electron microscopy (SEM). The surface topographies of the films were observed by atomic force microscopy (AFM) in an intermittent contact mode. Scanning transmission electron microscopy (STEM) was used to study the nanostructure. Cross-sectional lamellae for STEM work were prepared by ion beam milling using a combination of a focused high energy Ga ion beam and low energy Ar ion beam.[35] The atomic-resolution STEM imaging (HRSTEM) was done on a probe Cs-corrected Titan^3 G2 60-300 microscope operating at 300 kV accelerating voltage. A probe forming aperture of 25 mrad was used. Annular bright-field STEM images (ABF-STEM) were recorded with an annular detector using annular ranges of 10-19 mrad.

During the deposition of each film at different T_s, the crystalline quality of the surface was *in situ* monitored by means of RHEED. The clean unreconstructed Si substrates exhibit a streaky RHEED pattern with Kikuchi lines, as seen in Fig. 1(a). It reveals the high crystalline quality of the Si surfaces. Also, the chemical cleaning and etching processes of Si provide an oxide-free and smooth surface, which is desirable for the growth of an epitaxial thin film. For the films deposited at T_s ranging from RT to 100 °C, only diffuse RHEED patterns are observed (not shown). This demonstrates that within this temperature range, T_s is too low to promote a nucleation of crystallites. At T_s = 140 °C, a streaky pattern with low intensity started to appear for the as-deposited film (not shown).

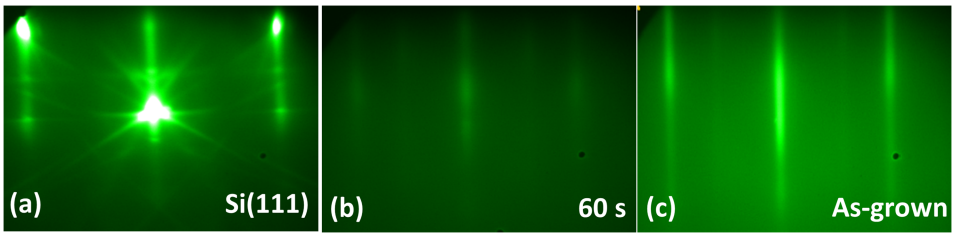

FIG. 1. RHEED patterns of (a) wet-chemically cleaned Si(111), (b) Sb_2Te_3 layers taken 60 s after deposition started, and (c) as-grown Sb_2Te_3 thin film deposited at 220 °C. The electron beam was parallel to <1-10> direction of the Si(111) substrate.

This indicates that this substrate temperature is sufficient to initiate the nucleation of crystalline regions.

Furthermore, for all the films deposited at $T_s \geq 160$ °C, the RHEED patterns are nearly identical, typically represented by Figs. 1(b) and 1(c), showing the RHEED pattern of the selected film deposited at 220 °C. The transition from the reflection of the substrate to that of the first layer of the film can be observed, as depicted by Fig. 1(b). The snapshot was taken 60 s after the deposition started, associated to ~1.3 nm of film thickness. In the figure, a sharp streaky intensity is observed, pointing out that the films are epitaxially grown with high crystallinity and a smooth surface morphology. A typical RHEED pattern of the as-deposited film can be seen in Fig. 1(c). The fact that a streaky pattern can be observed indicates that the as-grown films are smooth and have excellent surface crystallinity. Fig. 1(c) shows a diffraction pattern, which is identical to the one in Fig. 1(b), except that the intensity maxima are more pronounced.

As confirmed by XRR and SEM, the deposition rate was approximately constant (~1.3 nm/min) up to Ts = 230 °C (the film thickness of around 80 nm). However, the rate dropped dramatically for the film deposited at Ts ≥ 240 °C (the thicknesses are ~18 nm and ~12 nm for the films deposited at 240 and 260 °C, respectively). The surface topographies of as-deposited films were observed by means of AFM. Fig. 2 shows the selected as-deposited films, deposited at 220, 230, and 240 °C, respectively. The AFM measurements confirm that each film typically possesses a smooth surface. The root mean square (rms) roughness of all layers is less than 1 nm. Fine spiral-like structures with atomically smooth terraces are seen, especially in Fig. 2(b). This spiral-like structure was also observed on MBE-grown films.[36,37] For slightly higher deposition temperature (240 °C, Fig. 2(c)), the AFM measurement reveals the presence of atomically smooth terraces and steps, with a step height of 1 nm (1 quintuple layer). The spiral-like structures are almost not visible here. From these results, in connection with RHEED data, it can be assumed that, by means of PLD, epitaxial Sb_2Te_3 thin films typically grow in a two-dimensional growth mode. This layer-by-layer growth mode is desirable for a further outlook, i.e., the fabrication of a chalcogenide superlattice structure by means of PLD.

The crystalline structure and out-of-plane texture of Sb_2Te_3 thin films were investigated by measuring symmetrical 2θ-ω XRD scans. Fig. 3 shows 2θ-ω scans of the films deposited at different T_s from RT to 260 °C. The film deposited at RT, as shown by the black curve, shows only the

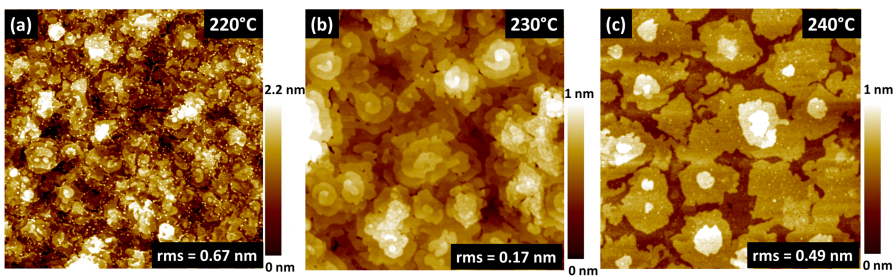

FIG. 2. AFM images of the as-deposited thin films. (a), (b), and (c) show the topographies of the films deposited at 220, 230, and 240 °C, respectively. All the figures are presented in 2 × 2 μm^2 scale.

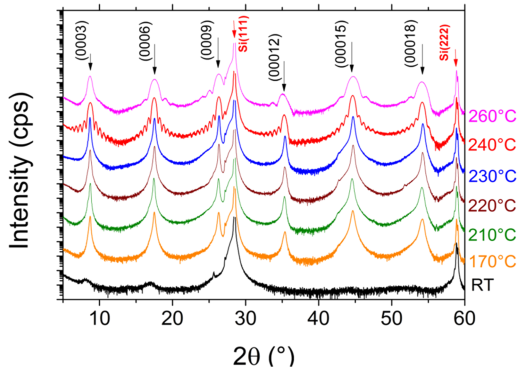

FIG. 3. 2θ-ω scans of Sb_2Te_3 deposited on Si(111) at different substrate temperatures T_s. The black curve belongs to the film deposited at RT, showing mainly amorphous phase. The curves belong to the films deposited at T_s = 170 °C until 260 °C all exhibit only Bragg reflections of trigonal Sb_2Te_3(000l). This shows that the films grow epitaxially in a trigonal crystal structure, according to (000l) out-of-plane orientation. The higher the T_s, the lower deposition rate, but the better crystalline quality.

amorphous structure, since there is no significant intensity peaks. However, the occurrence of small peaks situated at 8° and 17° which correspond to Sb_2Te_3(0003) and (0006) planes, respectively, indicates the presence of the trigonal phase. The next data to be presented in Fig. 3 are about the films deposited at T_s starting from 170 °C, showing only narrow and intense peaks which are associated to (000*l*) planes according to the calculated XRD spectra.[38,39] It points out that the films deposited within these temperatures possess a high crystalline quality. Special attention is on the film deposited at 240 °C. The film exhibits Laue fringes, showing that the film is homogeneous and possesses a high crystalline quality with a smooth surface. Above a deposition temperature of 260 °C, the process was dominated by surface desorption during the deposition, resulting in a lower deposition rate. From XRD it was found that the Sb_2Te_3 films are epitaxial with out-of-plane orientation of (000l). The out-of-plane epitaxial relationship is then determined to be Sb_2Te_3(0001) || Si(111). Using results of the XRD studies and the Scherrer relationship, the average grain size was determined to be 55 nm, which is in a good agreement with the lateral grain sizes between 47 nm and 107 nm obtained from cross section TEM images (not shown).

The crystalline qualities and in-plane epitaxial relation between the film and the substrate are investigated by measuring the in-plane pole figures. These ex-situ measurements are also to confirm the epitaxial window previously determined by *in situ* RHEED measurement. Figs. 4(a) and

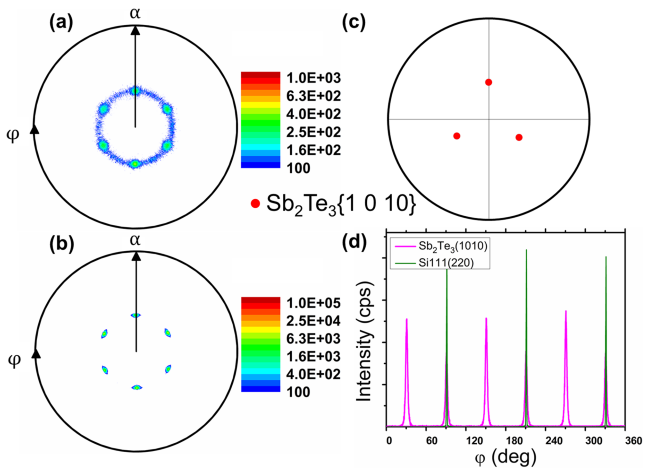

FIG. 4. In-plane pole figures of the Sb_2Te_3{1 0 10} reflections, for the films deposited at (a) 130 °C and (b) 220 °C. In (c), stereographic projection of model Sb_2Te_3{1 0 10} is presented. Thin film in (a) shows six (three times two) pole density maxima accompanied by intensity ring, while in (b), the intensity ring disappeared, while six pole density intensities are much more intense. (d) shows azimuthal scan of Sb_2Te_3{1 0 10} and Si{220} of the sample in (b).

4(b) present the pole figures of $Sb_2Te_3\{1\ 0\ 10\}$ reflections for the films deposited at 130 °C and 220 °C, respectively. The in-plane pole figure of the film deposited at 130 °C shows six, i.e., two times three, pole density maxima. The azimuthal angular distance between two neighboring maxima is 60°. These maxima are accompanied by a ring of low intensity connecting adjacent pole density maxima. The presence of this ring indicates a fiber oriented growth of the polycrystalline film.

For the film deposited at 220 °C, only those six pole density maxima remain and the ring intensity is not present anymore, as depicted by Fig. 4(b). This indicates that the film grows strictly epitaxial on Si. The small widths of the pole density intensity distribution for the polar and azimuth angles point out the high quality of the epitaxial growth. The expected position of the diffraction maxima for Sb_2Te_3[38,39] was calculated and presented in a stereographic projection in Fig. 4(c). From this pole figure, it can be discerned that a high symmetry calculation of the trigonal Sb_2Te_3 crystal results in three peaks representing $Sb_2Te_3\{1\ 0\ 10\}$ reflections. It can be concluded that the presence of six, instead of three, pole density maxima in the experimental data points out the presence of a twin domain. Such twin was also observed in the other epitaxial Te-based PCM, i.e., GST.[19,20] The intensity maxima in the calculated (Fig. 4(c)) as well as in the measured pole figures (Figs. 4(a) and 4(b)) are situated at $\alpha \approx 39°$. The azimuthal full width half maximum (FWHM) of the Sb_2Te_3 peak is around 3.5°. This indicates the presence of domain rotation in a small angle, due to a domain epitaxy of a highly mismatched epilayer. To determine the in-plane epitaxial relationship, a $Si\{220\}$ azimuthal φ-scan was performed (see Fig. 4(d)). The green curve is the φ-scan of $Si\{220\}$, while the magenta curve corresponds to $Sb_2Te_3\{1\ 0\ 10\}$ reflections. The in-plane epitaxial relationship is determined to be $Sb_2Te_3[2\text{-}1\text{-}10] \parallel Si[1\text{-}10]$.

High resolution scanning transmission electron microscopy (HRSTEM) was used to directly observe the microstructure and the atomic order in the Sb_2Te_3 thin films and their interfaces. Fig. 5 shows HRSTEM images of the Sb_2Te_3 thin film deposited at 240 °C. Fig. 5(a) depicts the presence of a single atomic layer of Sb/Te at the Sb_2Te_3-Si(111) interface, as indicated by the orange arrow on the left-hand side of Fig. 5(a). This points out that the Sb_2Te_3 growth is initiated by a Sb/Te surface passivation layer on the Si substrate. Due to almost a similar Z number and scattering cross sections of Sb and Te, the passivation layer is assumed to be a mixture of Sb and Te atomic species. The results of atom probe tomography performed on Sb_2Te_3 and Bi_2Te_3 multilayers grown on Si also showed an intermixing of Sb and Te at the interface.[36,37] The Sb/Te surface passivation layer was also observed in layered GST grown on Si by PLD.[20] The formation of a surface termination layer is well known to overcome a large lattice mismatch between the substrate and the thin film in vdW epitaxy[15] and was observed for different materials. Through that mechanism, hence, vdW epitaxy is achieved rather than lattice-matched (strained) epitaxy, resulting in a fully relaxed film lattice, even on a highly mismatched substrate. A similar effect was also reported for the deposited Sb_2Te_3 film,[11,12,40] in which Sb or Bi adsorption or deposition on Si is necessary prior to the thin film deposition. Interestingly,

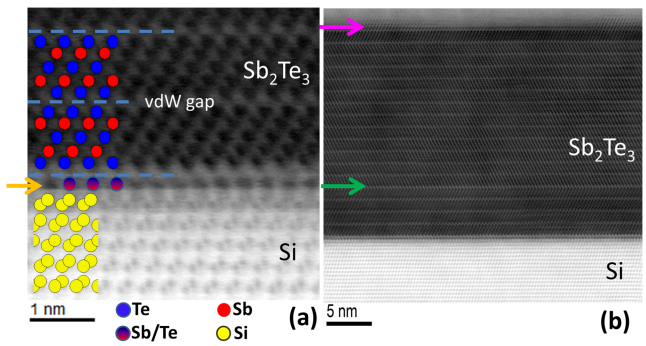

FIG. 5. ABF-STEM cross section images of thin Sb_2Te_3 film deposited at 240 °C. (a) shows a formation of Sb/Te-passivation layer, as marked by the orange arrow, at the Sb_2Te_3-Si(111) interface. The model Sb_2Te_3 and Si crystal (view in Si[-110] direction) are also presented. The dashed lines mark the quasi vdW gaps. (b) presents the HRSTEM image of the same sample in wider scale. The presence of defects (twins) is observed, as marked by the green arrow. The film thickness is around 17-18 units of Sb_2Te_3 building blocks (18 nm).

however, in the case of the epitaxy of the layered material Sb_2Te_3 by PLD, the termination of the dangling bonds at the Si surface is naturally accomplished within Sb_2Te_3 deposition without any pre-treatment (Si surface reconstruction followed Sb/Te-dangling bond termination) of the substrate. The explanation is that the pulsed laser ablated plasma contains the mixtures of atomic and ionic species as well as clusters. The formation of Sb/Te termination layer formed by the ambient Sb/Te vapor is energetically favorable in order to avoid a high stress/strain in the lattice of the growing thin film.

In Fig. 5, the quintuple layers (2Sb and 3Te), which are the characteristic for the Sb_2Te_3 crystal, can be clearly seen. This confirms the stoichiometric preservation in the Sb_2Te_3 thin film epitaxially grown by PLD. Analyzing intensities, the stacking sequence of a single QL is determined to be Te-Sb-Te-Sb-Te-vdW along the c-axis. Each two neighboring quintuple layer building blocks (Te-Te stacking layers) is intercalated by a quasi van-der-Waals gap. The dashed lines mark out the vdW gaps, which are present on the interface and in the Sb_2Te_3 bulk. The presence of such a 2D crystal structure of Sb_2Te_3 is due to an electron excess possessed by Sb atoms, so that the outermost Te-stacking layers of a building block are passivated.[41] This 2D crystal structure with vdW gaps was also found in other class of materials.[22–25] The corresponding crystal models[38,39] of Sb_2Te_3 and Si at the interface are also presented. The viewing direction is in Si[-110]. The Te, Sb, and Si are presented in blue, red, and yellow, respectively. The gradual color represents the mixture of Sb/Te. Fig. 5(b) presents a HRSTEM image in wider scale of the same sample. The 17-18 quintuple layers are observed, corresponding to a film thickness of around 18 nm, in agreement to the x-ray reflectivity measurement (not shown here). The presence of defects (twin boundaries) is also revealed, which is in agreement to the in-plane pole figures, as presented in Fig. 4. One example of this twin boundary is pointed out by the green arrow at the left-hand side of Fig. 5(b). Additionally, some mounds are characterized on the thin film surface, as pointed out by the purple arrow in Fig. 5(b). These mounds have maximum heights of around a single unit of a Sb_2Te_3 building block (1 nm), which is consistent with the AFM images. From this it can be concluded that the Sb_2Te_3 film is typically grown on Si(111) by PLD two-dimensionally by a stacking of Sb-Te quintuple layers.

To summarize, stoichiometric epitaxial Sb_2Te_3 thin films have been successfully grown on wet-chemically cleaned Si(111) substrates by PLD. Epitaxial growth is achieved for the films deposited at the temperature range between 140 and 280 °C. The best Sb_2Te_3 thin film was produced at T_s = 240 °C. Smooth film topographies with a maximum roughness of 1 QL (1 nm) are typically observed for as-deposited Sb_2Te_3 thin films. The Sb_2Te_3 thin films were grown on Si determined to follow a layer-by-layer growth mode, by a stacking of Sb-Te quintuple layers. The film possesses a trigonal crystal structure with (0001) out of plane orientation. The growth of Sb_2Te_3 thin films is initiated by the self-organized formation of a Sb/Te single-atomic passivation layer on the Si surface. The crystalline Sb_2Te_3 structure is built of quintuple layer building blocks, in which quasi vdW-bonding intercalates every two building blocks.

Isom Hilmi is grateful to Deutscher Akademischer Austauschdienst (DAAD) for the fellowship program. The authors also acknowledge A. Mill for TEM specimen preparation.

[1] D. Lencer, M. Salinga, B. Grabowski, T. Hickel, J. Neugebauer, and M. Wuttig, Nat. Mater. **7**, 972 (2008).
[2] R. Simpson, P. Fons, A. Kolobov, T. Fukaya, M. Krbal, T. Yagi, and J. Tominaga, Nat. Nanotechnol. **6**, 501 (2011).
[3] A. K. Geim and I. V. Grigorieva, Nature **499**, 419 (2013).
[4] M. Hase, P. Fons, K. Mitrofanov, A. V. Kolobov, and J. Tominaga, Nat. Commun. **6**, 8367 (2015).
[5] X. Zhou, J. Kalikka, X. Ji, L. Wu, Z. Song, and R. E. Simpson, Adv. Mater. **28**, 3007 (2016).
[6] D. Bang, H. Awano, J. Tominaga, A. V. Kolobov, P. Fons, Y. Saito, K. Makino, T. Nakano, M. Hase, Y. Takagaki *et al.*, Sci. Rep. **4**, 5727 (2014).
[7] Y. Saito, P. Fons, A. V. Kolobov, and J. Tominaga, Phys. Status Solidi B **252**, 2151 (2015).
[8] D. Kong, Y. Chen, J. J. Cha, Q. Zhang, J. G. Analytis, K. Lai, Y. Liu, S. S. Hong, K. J. Koski, S.-K. Mo *et al.*, Nat. Nanotechnol. **6**, 705 (2011).
[9] B. Huang, C. Lawrence, A. Gross, G.-S. Hwang, N. Ghafouri, S.-W. Lee, H. Kim, C.-P. Li, C. Uher, K. Najafi *et al.*, J. Appl. Phys. **104**, 113710 (2008).
[10] B. Saha, P. Chaturvedi, A. K. Yadav, D. Saha, and S. Ganguly, J. Vac. Sci. Technol., B **34**, 021806 (2016).
[11] G. Zhang, H. Qin, J. Teng, J. Guo, Q. Guo, X. Dai, Z. Fang, and K. Wu, Appl. Phys. Lett. **95**, 015114 (2009).
[12] J. E. Boschker, J. Momand, V. Bragaglia, R. Wang, K. Perumal, A. Giussani, B. J. Kooi, H. Riechert, and R. Calarco, Nano Lett. **14**, 3534 (2014).
[13] H. Li, Z. Wang, X. Kan, X. Guo, H. He, Z. Wang, J. Wang, T. Wong, N. Wang, and M. Xie, New J. Phys. **12**, 103038 (2010).

[14] N. Bansal, Y. S. Kim, E. Edrey, M. Brahlek, Y. Horibe, K. Iida, M. Tanimura, G.-H. Li, T. Feng, H.-D. Lee *et al.*, Thin Solid Films **520**, 224 (2011).
[15] A. Koma, Thin Solid Films **216**, 72 (1992).
[16] A. Richardella, D. Zhang, J. Lee, A. Koser, D. Rench, A. Yeats, B. Buckley, D. Awschalom, and N. Samarth, Appl. Phys. Lett. **97**, 262104 (2010).
[17] P. Tabor, C. Keenan, S. Urazhdin, and D. Lederman, Appl. Phys. Lett. **99**, 013111 (2011).
[18] G. Wang, L. Endicott, and C. Uher, Sci. Adv. Mater. **3**, 539 (2011).
[19] I. Hilmi, E. Thelander, P. Schumacher, J. Gerlach, and B. Rauschenbach, Thin Solid Films **619**, 81 (2016).
[20] I. Hilmi, A. Lotnyk, J. W. Gerlach, P. Schumacher, and B. Rauschenbach, Mater. Des. **115**, 138 (2017).
[21] U. Ross, A. Lotnyk, E. Thelander, and B. Rauschenbach, J. Alloys Compd. **676**, 582 (2016).
[22] Z. Yang and J. Hao, J. Mater. Chem. C **4**, 8859–8878 (2016).
[23] P. X. Feng and M. Sajjad, Mater. Lett. **89**, 206 (2012).
[24] M. Mahjouri-Samani, R. Gresback, M. Tian, K. Wang, A. A. Puretzky, C. M. Rouleau, G. Eres, I. N. Ivanov, K. Xiao, M. A. McGuire, G. Duscher, and D. B. Geohegan, Adv. Funct. Mater. **24**, 6365–6371 (2014).
[25] M. I. Serna, S. H. Yoo, S. Moreno, Y. Xi, J. P. Oviedo, H. Choi, H. N. Alshareef, M. J. Kim, M. Minary-Jolandan, and M. A. Quevedo-Lopez, ACS Nano **10**(6), 6054–6061 (2016).
[26] I. S. Virt, T. P. Shkumbatyuk, I. V. Kurilo, I. O. Rudyi, T. Ye. Lopatinskyi, L. F. Linnik, V. V. Tetyorkin, and A. G. Phedorov, Semiconductors **44**, 544 (2010).
[27] R. Venkatasubramanian, E. Siivola, T. Colpitts, and B. O'quinn, Nature **413**, 597 (2001).
[28] J. Momand, R. Wang, J. E. Boschker, M. A. Verheijen, R. Calarco, and B. J. Kooi, Nanoscale **7**, 19136 (2015).
[29] H. Zhang, C.-X. Liu, X.-L. Qi, X. Dai, Z. Fang, and S.-C. Zhang, Nat. Phys. **5**, 438 (2009).
[30] D. Hsieh, Y. Xia, D. Qian, L. Wray, F. Meier, J. Dil, J. Osterwalder, L. Patthey, A. Fedorov, H. Lin *et al.*, Phys. Rev. Lett. **103**, 146401 (2009).
[31] D. Wright, Nature **181**, 834 (1958).
[32] Y. Hor, A. Richardella, P. Roushan, Y. Xia, J. Checkelsky, A. Yazdani, M. Hasan, N. Ong, and R. Cava, Phys. Rev. B **79**, 195208 (2009).
[33] T. Ikeda, L. A. Collins, V. A. Ravi, F. S. Gascoin, S. M. Haile, and G. J. Snyder, Chem. Mater. **19**, 763 (2007).
[34] A. Lotnyk, U. Ross, S. Bernütz, E. Thelander, and B. Rauschenbach, Sci. Rep. **6**, 26724 (2016).
[35] A. Lotnyk, D. Poppitz, U. Ross, J. Gerlach, F. Frost, S. Bernütz, E. Thelander, and B. Rauschenbach, Microelectron. Reliab. **55**, 2119 (2015).
[36] M. Lanius, J. Kampmeier, Ch. Weyrich, S. Kölling, M. Schall, P. Schüffelgen, E. Neumann, M. Luysberg, G. Mussler, P. M. Koenraad, T. Schäpers, and D. Grützmacher, Cryst. Growth **16**, 2057–2061 (2016).
[37] M. Lanius, J. Kampmeier, S. Kölling, G. Mussler, P. M. Koenraad, and D. Grützmacher, J. Cryst. Growth **453** 158–162 (2016).
[38] See http://carine.crystallography.pagespro-orange.fr for CaRIne Crystallography Divergent S. A.
[39] T. L. Anderson and H. B. Krause, Acta Crystallogr., Sect. B: Struct. Crystallogr. Cryst. Chem. **30**, 1307 (1974).
[40] S. Andrieu, J. Appl. Phys. **69**, 1366 (1991).
[41] J. Momand, F. R. L. Lange, R. Wang, J. E. Boschker, M. A. Verheijen, R. Calarco, M. Wuttig, and B. J. Kooi, J. Mater. Res. **31**(20), 3115 (2016).